In vivo quantification of chromophore concentration using fluorescence differential path length spectroscopy

Bastiaan Kruijt
Slavka Kascakova
Henriette S. de Bruijn
Angelique van der Ploeg-van den Heuvel
Henricus J. C. M. Sterenborg
Dominic J. Robinson
Centre for Optical Diagnostics and Therapy
Department of Radiation Oncology
Erasmus MC Room Ee1675
P.O. Box 2040
3000 CA Rotterdam
The Netherlands

Arjen Amelink
Centre for Optical Diagnostics and Therapy
Department of Radiation Oncology
Erasmus MC Room Ee1675
P.O. Box 2040
3000 CA Rotterdam
The Netherlands
E-mail: a.amelink@erasmusmc.nl

Abstract. We present an optical method based on fluorescence spectroscopy for measuring chromophore concentrations *in vivo*. Fluorescence differential path length spectroscopy (FPDS) determines chromophore concentration based on the fluorescence intensity corrected for absorption. The concentration of the photosensitizer m-THPC (Foscan®) was studied *in vivo* in normal rat liver, which is highly vascularized and therefore highly absorbing. Concentration estimates of m-THPC measured by FDPS on the liver are compared with chemical extraction. Twenty-five rats were injected with 0.3 mg/kg m-THPC. *In vivo* optical concentration measurements were performed on tissue 3, 24, 48, and 96 h after m-THPC administration to yield a 10-fold variation in tissue concentration. After the optical measurements, the liver was harvested for chemical extraction. FDPS showed good correlation with chemical extraction. FDPS also showed a correlation between m-THPC fluorescence and blood volume fraction at the two shortest drug-light intervals. This suggests different compartmental localization of m-THPC for different drug-light intervals that can be resolved using fluorescence spectroscopy. Differences in measured m-THPC concentration between FDPS and chemical extraction are related to the interrogation volume of each technique; $\sim$0.2 mm^3 and $\sim 10^2$ mm^3, respectively. This indicates intra-animal variation in m-THPC distribution in the liver on the scale of the FDPS sampling volume. [DOI: 10.1117/1.3149862]

Keywords: chemical extraction; fluorescence spectroscopy; reflectance spectroscopy; optical concentration measurements.

Paper 08408R received Nov. 18, 2008; revised manuscript received Mar. 7, 2009; accepted for publication Apr. 3, 2009; published online Jun. 9, 2009.

1 Introduction

Noninvasive optical methods for measuring tissue concentrations of endogenous and exogenous substances have several benefits over invasive techniques. Most importantly, optical concentration measurements allow nondestructive *in vivo* monitoring of drug pharmacokinetics at various tissue sites.[1–5] Two different sources of optical contrast are routinely used for target compound concentration measurements in tissue: absorption and fluorescence.

Methods based on absorption (reflectance) spectroscopy have the advantage that the measurement setup is relatively simple compared to fluorescence measurements. A typical setup consists of a fiber-optic probe, a broadband light source, and a spectrometer. The signal analysis is based on attenuation of elastically scattered light. Integration times are generally small, which enables measurements in the presence of ambient lighting (e.g., endoscopic illumination) and allows continuous measurements with a high temporal resolution. The optical contrast depends on the product of path length and target compound absorption coefficient, where the latter is the product of molar extinction coefficient and concentration. This implies that the absorption contrast might become too low for accurate concentration measurements for short path lengths, small molar extinction coefficients, and small target compound concentrations. An additional problem arises when the absorption band of the target compound overlaps the absorption bands of highly absorbing endogenous chromophores such as blood. In that case, the attenuation of the scattered light due to blood might prevent accurate concentration estimates of the target compound as well.

For most fiber-optic measurement geometries, the optical path length depends on the scattering coefficient μ_s and on the absorption coefficient μ_a of the tissue. Since μ_s and μ_a both vary significantly in tissue, quantitative measurements prove to be difficult in tissue unless specific fiber-optic measurement geometries are chosen. For example, the optical pharmacokinetics spectroscopy (OPS) system developed by Mourant et al.[1] uses elastic scattering spectra of tissue to calculate the

Address all correspondence to Arjen Amelink, Radiation Oncology, Erasmus MC, PO Box 2040-Rotterdam, 3000 CA Netherlands. Tel: +31-10-7032104; Fax: +31-10-7032141; E-mail: a.amelink@erasmusmc.nl

1083-3668/2009/14(3)/034022/8/$25.00 © 2009 SPIE

concentration of chromophores in tissue using a fiber-optic probe with a source–detector separation of 1.7 mm. The separation of 1.7 mm was chosen to minimize the path length dependence of the collected photons on scattering properties of tissue. For scattering parameters that are typical of tissue, the path length varies by less than 20% for a given background absorption. Another technique that features a known path length is differential path length spectroscopy (DPS).[6–9] The path length of photons contributing to the differential reflectance signal varies by less than 20% over a very broad range of both scattering and absorption coefficients.[6,7] This facilitates quantitative concentration measurements even for strong variations in either background absorption or scattering. However, as explained earlier, chromophore concentration measurements based on attenuation of elastically scattered light rely on (small) differences between large amounts of detected light with and without the target chromophore present. Therefore, accurate measurement of small concentrations of chromophores or measurements of chromophores with low absorption coefficients are difficult. This is particularly true for DPS, for which the average path length of the measured photons is very small, approximately equal to the fiber diameter.[6–9] Moreover, for fluorescing compounds such as photosensitizers, the concentration can be underestimated due to the presence of fluorescence, induced by the lower wavelengths of the white-light source, in the reflection spectra.[4] For example, Johansson et al.[4] used the OPS technique to estimate m-THPC concentration in a nonmelanotic skin tumor model and found a factor 2 underestimation in m-THPC concentration when not accounting for the presence of m-THPC fluorescence.

In contrast, measurements based on fluorescence contrast rely on the induced fluorescence of the fluorescing compound. Furthermore, the dynamic range for measurements based on fluorescence contrast is much larger than for scattering (absorption) measurements since the fluorescence is measured at a different wavelength than the excitation (scattered) light. Therefore, fluorescence-based concentration measurements are more sensitive and better capable of measuring very low fluorophore concentrations simply by increasing the integration time. However, there exists a complex relationship between the concentration of a chromophore and its absorption cross section and fluorescence emission intensity. *In vivo* fluorescence can be influenced by many factors that include changes in quantum yield induced by changes in the microenvironment,[10] photobleaching,[11] biological compartmentalization, and alteration in binding and aggregation.[12,13] In a turbid sample, the amount of fluorescence detected depends not only on the fluorophore concentration and quantum yield, but also on the scattering and absorption coefficients of the sample at the excitation and emission wavelengths. Various algorithms and measurement geometries have been developed to correct for the influence of tissue optical properties on a measured fluorescence spectrum. Photon migration techniques have been used to establish a general algorithm, applicable to any measurement geometry and for a broad range of scattering and absorption variations, to correct the measured fluorescence for the influence of tissue optical properties.[14,15] For this algorithm, the diffuse reflectance is measured in the same geometry as the fluorescence measurements and used to correct for differences in optical properties. However, elaborate probe-specific calibration procedures are required, and the correction algorithm itself is quite complex. Several other more simple correction algorithms based on specific probe geometries have been developed.[16–19] We have recently developed fluorescence differential path length spectroscopy (FDPS), which is based on the principles of DPS (the difference of two signals that contain the same contribution from long path length photons but different contributions from short path length photons, to obtain a well-defined, small measurement volume) but with the enhanced dynamic range of fluorescence measurements.[5] The advantage of FDPS over other quantitative fluorescence measurements is its capability to deal with large variations in background absorption using a simple correction algorithm.

In this paper, we compare an optical concentration measurement technique based on quantitative fluorescence spectroscopy, FDPS, with chemical extraction.[20] The photosensitiser m-THPC was chosen as the target chromophore to test the concept of FDPS *in vivo*. To test the strength of FDPS *in vivo*, we performed the measurements on highly absorbing tissue, the liver. Variations in m-THPC concentration in the liver are achieved by choosing different drug-light intervals based on the known pharmacokinetics of m-THPC in liver.[21,22] The distribution of m-THPC at the different time points within the liver was investigated using fluorescence microscopy.

2 Materials and Methods

2.1 *Animal and Measurement Procedures*

The experimental design for this study was approved by the animal experiment committee of the Erasmus MC. Two weeks before the start of the experiments, 25 normal adult male Wistar rats were placed on a diet of chlorophyll-free food to minimize the influence on autofluorescence centered at 675 nm due to pheophorbide-α. All rats were injected with 0.3 mg/kg m-THPC i.v., except for the control animals ($n=5$), which were injected with the solution (PEG400:ethanol:water, 2:3:5) not containing m-THPC. At either 3 h, 24 h, 48 h, or 96 h after injection ($n=5$ animals per time point), the tissue overlying the liver was dissected, and optical concentration measurements were conducted on 10 randomly chosen positions across different lobes of the liver. Directly after the optical measurements, the main arteries and veins of the liver were clamped to minimize the loss of blood. The liver was then excised and snap-frozen in liquid nitrogen.

2.2 *Concentration Measurements*

Concentration of m-THPC in the liver was measured *in vivo* using FDPS and *ex vivo* using chemical extraction. FDPS determines a concentration estimate based on the emitted photosensitizer fluorescence. Figure 1 shows a schematic diagram of the measurement setup. The concentration estimates measured by FDPS were compared to the concentration values determined by chemical extraction. Both methods, FDPS and chemical extraction, are described in more detail in the following sections.

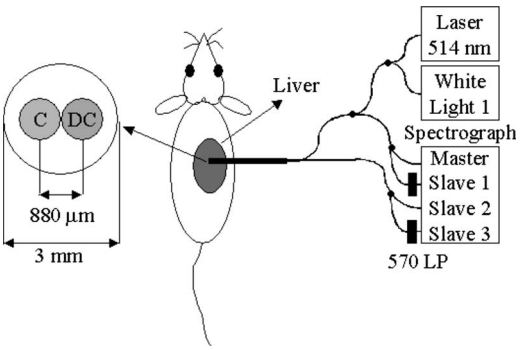

Fig. 1 Schematic diagram of the FDPS measurement setup. The probe tip with a diameter of 3 mm contains two 800-μm fibers at a core-to-core distance of 880 μm.

2.2.1 *FDPS*

The probe contained two 800-μm fibers placed at minimum core-to-core distance, 880 μm, in a specially adapted subminiature version A (SMA) connector. The SMA connector configuration ensured a reproducible fixed distance when calibrating the setup using a calibration lamp, as described elsewhere.[5] The probe surface was polished under an angle of 15 deg to minimize specular reflections at the probe-medium interface during FDPS measurements. The 800-μm delivery-and-collection (dc) fiber is coupled into a 400-μm bifurcated fiber, which contains a delivery and a collection leg. The delivery leg is coupled into a 200-μm bifurcated fiber, of which one end is coupled into a xenon light source (HPX-2000, Ocean Optics, Duiven, The Netherlands) and the other end to a 514-nm argon laser (Spectra Physics, Eindhoven, The Netherlands). The collection leg is also coupled into a 200-μm bifurcated fiber, of which one end directly leads to the first channel of a temperature-regulated four-channel spectrograph setup (MC-2000-4-TR2, Ocean Optics, Duiven, The Netherlands) and the other end leads to a filter block containing a 570-nm long-pass filter before being coupled into the second channel of the spectrograph. The 800-μm collection (c) fiber is coupled to a 400-μm bifurcated fiber, of which one end directly leads to the third channel and the other is again first filtered by the same 570-nm long-pass filter before being coupled in the fourth spectrograph channel.

2.2.2 *Tissue extraction*

Tissue extraction was performed according to the chemical extraction method recently described by Kascáková et al.[20] This is a modification of the original method described by Lilge et al.[23] In short, small liver tissue samples ($\sim$0.1 grams or $\sim$100 mm^3) were randomly acquired from the liver. Note that we did not attempt to colocate the optical measurement sites with the tissue extraction sites. Instead, we avoided complicated experimental procedures associated with colocating the sites by averaging multiple random locations in both the optical and chemical concentration measurements. The liver samples were dissolved in 2 ml of the ready-to-use tissue solvent Solvable™ (Perkin Elmer, Groningen, The Netherlands), which is a mixture of dodecyldimethylamine oxide (2.5 to 10%), secondary alcohol ethoxylate (2.5 to 10%), and sodium hydroxide ($\leqslant$2.5%) in water. Subsequently, the tissue sample in Solvable was placed in a water bath of 50°C and agitated regularly for 2 h. The solubilized liver solution was then diluted with Solvable to an OD$<$0.1, to minimize absorption artifacts and to ensure homogenous illumination of the sample in 1-cm path length quartz cuvettes in a fluorimeter (Perkin Elmer, Groningen, The Netherlands). The diluted samples were analyzed by using an excitation wavelength of 423 nm (corresponding to the wavelength at which m-THPC in 100% Solvable absorbs the most[20]) and a spectral detection band of 450 to 800 nm with a resolution of 0.5 nm.

2.3 *Fluorescence Microscopy*

Frozen tissue samples of control and m-THPC administered animals were handled under subdued light conditions. Liver sections of 20-μm thickness were sectioned and mounted on glass slides (Menzel, Braunschwig, Germany). Fluorescence images were acquired at a 50$\times$ magnification using a CCD camera (ORCA-ER, Hamamatsu, Herrsching am Ammersee, Germany) mounted on a fluorescence microscope (Leica, Leiden, The Netherlands) equipped with an N2.1 filter block with an additional bandpass detection filter, 670$\pm$50 nm.

2.4 *Data Processing*

2.4.1 *FDPS*

Before every measurement, the FDPS system was calibrated as described previously.[5] A differential reflectance spectrum (DPS) is obtained by subtracting the spectral signal from the c-fiber, which collects long path length photons only, from the dc-fiber, which collects photons of both long and short path length. Hence, the differential spectrum contains the spectral contribution from short path length photons only. Differential reflectance spectra were fitted according to the following model[6–9,24]:

$$R = \left[a_1 \left(\frac{\lambda}{\lambda_0} \right)^{a2} + a_3 \left(\frac{\lambda}{\lambda_0} \right)^{-4} \right] \cdot \exp\{ - d_{fiber} \cdot \rho \cdot [StO_2 \cdot \mu_a^{HbO_2}(\lambda) + (1 - StO_2) \cdot \mu_a^{Hb}(\lambda)] \cdot C_{cor}(D_{ves}) \cdot C_{cor}(\mu_a^{total}) \}. \quad (1)$$

The scattering function is modeled by a combination of Mie scattering and Rayleigh scattering, given by power law functions with amplitudes a_1 and a_3 and wavelength dependencies $(\lambda/\lambda_0)^{a_2}$ and $(\lambda/\lambda_0)^{-4}$, respectively. Here, λ_0 is a normalization wavelength where the signal is predominantly dependent on scattering, which we usually set to 800 nm. d_{fiber} is the fiber diameter (0.8 mm), ρ is the blood volume fraction, StO_2 is the microvascular blood oxygenation, $\mu_a^{\mathrm{HbO2}}(\lambda)$ is the absorption coefficient of fully oxygenated whole blood, and $\mu_a^{\mathrm{Hb}}(\lambda)$ is the absorption coefficient of fully deoxygenated whole blood.[25] $C_{cor}(D_{ves})$ is a correction factor that accounts for the inhomogeneous distribution of blood in tissue and depends on the vessel diameter D_{ves}, and $C_{cor}(\mu_a^{\mathrm{total}})$ is a correction factor that accounts for the absorption dependence of the path length for highly vascularized tissue such as liver.[26] A differential fluorescence spectrum (DF_{meas}) is obtained by subtracting the fluorescence spectral signal measured by the c-fiber from the fluorescence spectral signal measured by the dc-fiber. The measured differential fluorescence signal is cor-

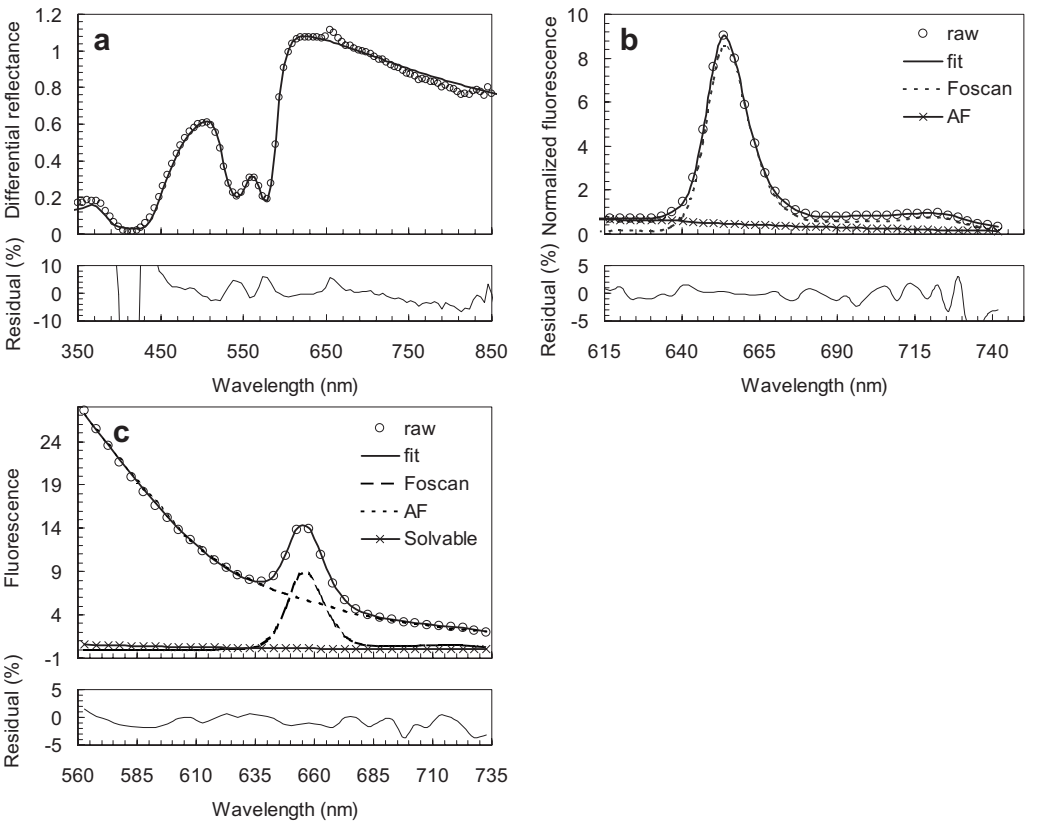

Fig. 2 Typical Levenberg-Marquardt fit of the DPS signal (a) and SVD fit for the FDPS signal (b) acquired under 514-nm excitation. (c) SVD fit for the fluorescence signal of the liver after chemical extraction measured using a fluorimeter.

rected for absorption by multiplying DF_{meas} by the ratio of the reflectance at the excitation wavelength without and with absorption present, as follows[5]:

$$DF_{corr} = DF_{meas}\frac{DR_x(0)}{DR_x(\mu_{a,x})}, \quad (2)$$

where $DR_x(\mu_{a,x})$ and $DR_x(0)$ are the differential reflectance signals at the excitation wavelength measured with and without background absorber present, respectively. $DR_x(\mu_{a,x})$ is the DPS signal at the excitation wavelength measured *in vivo*. The DPS signal at the excitation wavelength without absorption present, $DR_x(0)$, cannot be measured, but is calculated from the fit of the *in vivo* DPS spectrum to Eq. (1), using the best estimates of the parameters a_1 to a_3 and setting the exponent for the exponential term to 0. It was previously shown that the differential fluorescence signal is relatively insensitive to variations in scattering,[5] and consequently no corrections were performed to account for scattering differences between tissue samples. The absorption-corrected FDPS spectra were analyzed as a linear combination of basis spectra and fitted using a singular value decomposition (SVD) algorithm.[24,27] The fluorescence was described by a combination of autofluorescence and m-THPC fluorescence. Basis spectra for these two components were extracted from spectra acquired *in vivo*. The autofluorescence basis spectrum is the normalized average of the control animals. For m-THPC, a basis spectrum, based on the spectra acquired *in vivo* corrected for the autofluorescence, is determined for each of the four time points to account for possible spectral changes in m-THPC fluorescence due to changes in environment and/or binding.

2.4.2 *Chemical extraction*

Fluorescence spectra acquired by the fluorimeter could be described as a linear combination of autofluorescence, Solvable fluorescence, and m-THPC fluorescence. The Solvable fluorescence basis spectrum was measured in the fluorimeter using pure Solvable. m-THPC was dissolved in Solvable and measured in the fluorimeter; the basis spectrum for m-THPC was acquired by subtracting the Solvable component. Last, the autofluorescence basis spectrum is the normalized average fluorescence spectrum of spectra acquired from dissolved liver samples of control animals after subtraction of the Solvable component. The absolute m-THPC concentration of the liver samples was derived from a calibration curve, which was constructed from measurements of known m-THPC concentrations mixed with dissolved control liver samples in Solvable.[20]

2.5 *Statistics and Correlation*

Confidence intervals on the individual parameters for the individual measurements were determined based on the covariance matrix generated for each fit as described by Amelink et al.[28] Differences between groups were determined using the nonparametric Mann-Whitney test.

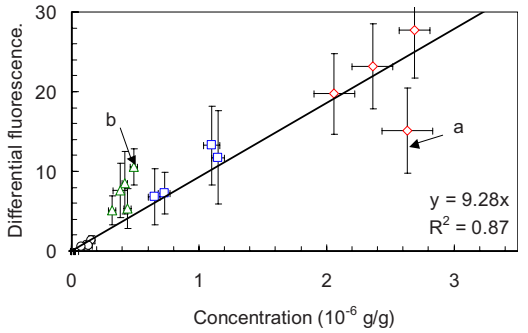

Fig. 3 Optically measured m-THPC concentration using FDPS versus true m-THPC concentration measured by chemical extraction for the four different time points 3 h (◇), 24 h (□), 48 h (△), and 96 h (○), together with the regression line.

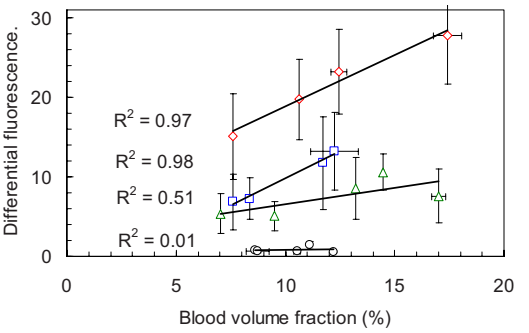

Fig. 4 Optically measured concentration using FDPS as a function of DPS-measured blood volume fraction averaged per animal for the four different time points 3 h (◇), 24 h (□), 48 h (△), and 96 h (○).

3 Results

Figure 2 shows the data and fit for the three spectra acquired per animal for the different methods: DPS, FDPS, and chemical extraction. Figure 2(a) shows a typical differential reflectance spectrum acquired *in vivo* from rat liver with its fit and residual between fit and data from an animal 3 h after m-THPC injection. Figure 2(b) shows the fit of a differential fluorescence spectrum acquired *in vivo* under 514-nm excitation of the rat liver 24 h after m-THPC injection. In addition to the fit and residual between fit and data, the individual components are also shown. Figure 2(c) shows a typical fluorescence spectrum and its fit and the individual components (m-THPC, autofluorescence, and Solvable fluorescence) of extracted liver tissue 3 h after m-THPC injection measured using the fluorimeter at 423-nm excitation.

Figure 3 shows the m-THPC component of the absorption-corrected FDPS fluorescence versus the actual m-THPC concentration determined with chemical extraction. For the control animals, the FDPS spectrum was fully described by the autofluorescence component with negligible contribution from the m-THPC component, as expected. The smallest non-zero amount of m-THPC fluorescence (measured at the 96-h time point) corresponded to an actual m-THPC concentration of 160 ng/g. Fitting a straight line forced through the origin shows an R^2 value of 0.87. Every measurement point represents the average of multiple fluorescence measurements at randomly chosen locations on the liver in a single animal. For these animals, the average blood volume fraction, measured with DPS, was $11.1 \pm 3\%$. The two most prominent average deviations from the straight line, indicated by arrows *a* and *b* in Fig. 3, had an average blood volume fraction of $7.6 \pm 0.02\%$ and $14.5 \pm 0.05\%$, respectively. Furthermore, all animals in the 48-h group are above the regression line in Fig. 4. The three animals within this group that deviate from the regression line by more than one times the standard deviation show an increased blood volume fraction ($14.9 \pm 2\%$) compared to the total average blood volume fraction for all animals ($11.1 \pm 3\%$). These observations indicate a possible relationship between measured m-THPC fluorescence and blood volume fraction. In Fig. 4, therefore, we have plotted the m-THPC fluorescence intensity as a function of blood volume fraction for each animal. Indeed a strong correlation between m-THPC fluorescence and blood volume fraction is observed for the early time points, 3 and 24 h. A decrease in correlation coefficients between m-THPC fluorescence and blood volume fraction with increasing drug-light intervals is observed.

Another interesting feature to be noticed in Fig. 3 is the difference in standard deviations between FDPS intensity and m-THPC concentration determined through chemical extraction. The large standard deviations in FDPS intensity are caused by intra-animal variations in m-THPC fluorescence in the liver, most likely related to a heterogenous distribution of m-THPC on a scale resolved by the FDPS technique but averaged out in the extraction. Therefore, we investigated the m-THPC fluorescence distribution at the different time points in liver sections using fluorescence microscopy. Figure 5 shows representative fluorescence microscopy images at 50 × magnification of liver sections for the 3-, 24-, 48-, and 96-h time points. The 3-h time point clearly shows intense clusters of m-THPC fluorescence randomly spread throughout the section. At 24 h, m-THPC fluorescence is measured in the whole section, and more intense m-THPC fluorescence is observed around the bigger vessels, which appear black in the image due to blood absorption. The 48-h animal shows similar m-THPC fluorescence distribution as on the 24-h time point, with the difference that the overall m-THPC fluores-

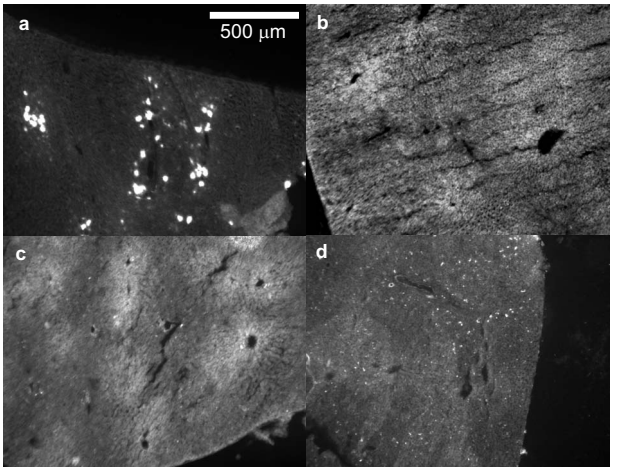

Fig. 5 Fluorescence microscopy performed on 20-μm thick liver sections at 50× magnification for the (a) 3 h, (b) 24 h, (c) 48 h, and (d) 96 h time points.

cence intensities are lower. The 96-h time point shows m-THPC fluorescence more evenly distributed throughout the section than on the other time points.

4 Discussion

The aim of this study was to test the concept of optical concentration measurements based on quantitative fluorescence spectroscopy (FDPS) *in vivo*. We have chosen to validate the FDPS concentration measurements in an *in vivo* environment on highly vascularized and thus highly absorbing tissue (liver) using m-THPC as an exogenous chromophore. Different drug-light intervals were chosen based on the pharmacokinetics of m-THPC in the liver[21,22] to vary the *in vivo* tissue concentrations by an order of magnitude. FDPS concentration estimates for the different time points were compared with chemical extraction.

Based on our measurements, we found that FDPS is capable of measuring m-THPC concentrations as low as 160 ng/g in the liver at the 96-h drug-light interval. We expect to be able to measure even lower concentrations by optimizing the setup and increasing the integration time. The measured m-THPC concentration with FDPS showed good linear correlation with the extracted m-THPC concentration, $R^2=0.87$. The correlation coefficient could be improved to 0.96 when the outliers from the linear regression line in Fig. 3, identified as *a* and *b*, are omitted. However, these outliers yield important information about *in vivo* m-THPC localization. The animals with the two most prominent deviations from the straight line, indicated by arrows *a* and *b*, were shown to have blood volume fractions of $7.6\pm0.02\%$ and $14.5\pm0.05\%$, respectively. These are significantly different from the average blood volume fraction of the m-THPC animals, $11.1\pm3\%$. (The blood volume fraction of the control animals was $9.1\pm4\%$, which is not significantly different from the m-THPC animals.) Based on this observation, we investigated the correlation between m-THPC concentration measured using FDPS and blood volume fraction. For the two shortest drug-light intervals, we found a strong correlation (R^2 values of 0.97 and 0.98 for the 3-and 24-h drug-light intervals). For longer drug-light intervals, there was a decrease in the correlation between m-THPC fluorescence intensity and blood volume fraction. The drug-light interval dependence of the correlation between fluorescence and blood volume suggests that m-THPC is predominantly localized in or near the tissue vasculature for short drug-light intervals and less so for longer drug-light intervals. This is in agreement with a range of m-THPC pharmacokinetic studies in rats showing high concentrations of m-THPC in the plasma directly after i.v. injection, followed by an initial rapid exponential decrease followed by one or two exponential decays with lower elimination rates.[21,22]

Another interesting observation is that the intra-animal variations in FDPS signals are up to a factor of 5 larger than those of chemical extraction. The source for these larger variations in FDPS concentration estimates is potentially related to (intra-animal) differences in tissue scattering, since the FDPS signal is dependent on scattering. The scattering dependence of the FDPS signal depends on the probe geometry. For an 800-μm FDPS probe, it has been shown in a phantom study that within biological relevant scattering values, the FDPS signal can vary by a factor of 2.2 (Ref. 5). Since in these experiments the overall variation in the scattering parameter (a_1) was small, 16%, it is safe to assume that scattering had no significant influence on the FDPS signal and hence does not contribute to the variation in the data, inter-or intra-individual. It is most likely that the differences in standard deviations between FDPS and chemical extraction are related to intra-animal variability in m-THPC concentration on a microscopic scale and are a result of the different interrogation volumes of the techniques. For chemical extraction, tissue samples of $\sim10^2$ mm^3 are used, whereas FDPS probes only ~0.2 mm^3 of tissue [corresponding to the volume of a cylinder with a diameter equal to the fiber (0.8 mm) and height of half the path length (0.4 mm)]. Fluorescence microscopy on sections at $50\times$ magnification for the four different time points (Fig. 5) shows a heterogeneous m-THPC fluorescence distribution throughout the sections. This heterogeneous distribution of m-THPC is on a submillimeter spatial scale and can be picked up only by techniques that sample small tissue volumes. Obviously, the tissue volumes used for chemical extraction are too large to pick up this submillimeter spatial heterogeneity, and standard deviations in m-THPC concentrations are small since multiple regimes of high and low fluorescence are present in each individual tissue volume used for chemical extraction. However, the measured m-THPC fluorescence intensity using FDPS depends heavily on probe placement on the liver; some measurements will contain bright spots of fluorescence, and other measurements on the same liver will contain smaller amounts of m-THPC, leading to large intra-animal variations in fluorescence intensity.

The spatial m-THPC distribution in the liver at different time points using fluorescence microscopy [Fig. 5(a)] illustrates the wide variations in spatial distribution of m-THPC in rat liver 3 h after the administration of m-THPC. It is clear that the localization of m-THPC is not coincident with the whole liver vasculature and that depending on probe placement, the volume interrogated by our optical technique contains areas of very high or low m-THPC fluorescence intensities. The spatial distribution of m-THPC is likely to be dominated by the role of the liver in the elimination of m-THPC.[29,30] A number of studies have illustrated the complexity of m-THPC pharmacokinetics *in vivo*.[21,31,32] These studies have shown the formation of m-THPC aggregates and the importance of binding to plasma proteins. Jones et al.[21] postulated that m-THPC could disaggregate and redistribute to lipoproteins in the liver before further distribution to other tissues. It is therefore not surprising that m-THPC fluorescence is not homogeneously distributed within the liver vasculature 3 h after the administration of m-THPC. In the liver, we observe increased m-THPC fluorescence around the vascalature at both intermediate (24 h) and long drug-light intervals (48 h and 96 h). Note that m-THPC fluorescence is observed throughout the whole section, although in a lower intensity than around the vasculature.

Another important consideration is that the measured fluorescence signal by FDPS is the product of the photosensitizer concentration and the quantum yield. The quantum yield of a photosensitizer can change due to changes in environment and binding[10,12,13] and might give a possible indication on

(sub)cellular localization of the photosensitizer. We find a linear correlation between FDPS measured fluorescence and extracted concentration, which suggests that the quantum yield is relatively constant over the drug-light intervals that we have investigated. This observation is in agreement with the fact that we found only small differences in the shape of the basis spectra for different m-THPC drug-light intervals (data not shown). It seems that these binding effects are not sufficiently large to affect the m-THPC concentration estimate. We note that there may be subtle differences in quantum yield with respect to drug-light interval in the liver and that other organs might show significant variations in quantum yield. It should also be noted that steady-state fluorescence measurements are rather insensitive to the effects of binding and variations in quantum yield and that time-resolved spectroscopy would be much more appropriate to determine the magnitude of these effects.[33,34] The possible subtle differences in fluorescence quantum yield and the differences in scattering properties for different tissue types strongly suggest the necessity to determine a calibration curve (such as Fig. 3 for liver) for each tissue type separately. This is a topic currently under investigation.

In conclusion, we compared an optical concentration measurement technique based on quantitative fluorescence spectroscopy (FDPS) with chemical extraction in an *in vivo* model. FDPS showed good correlation with chemical extraction and an ability to measure m-THPC values as low as 160 ng/g. Moreover, for short drug-light intervals, a correlation was observed between blood volume fraction and measured m-THPC fluorescence. A larger intra-animal variability was measured with FDPS compared to chemical exctraction due to its smaller interrogation volume and heterogenous distribution of m-THPC on the scale of the FDPS sampling volume.

References

1. J. R. Mourant, T. M. Johnson, G. Los, and I. J. Bigio, "Noninvasive measurement of chemotherapy drug concentrations in tissue: preliminary demonstrations of *in vivo* measurements," *Phys. Med. Biol.* **44**(5), 1397–1417 (1999).
2. S. C. Kanick, J. L. Eiseman, E. Joseph, J. Guo, and R. S. Parker, "Noninvasive and nondestructive optical spectroscopic measurement of motexafin gadolinium in mouse tissues: comparison to high-performance liquid chromatography," *J. Photochem. Photobiol., B* **88**(2–3), 90–104 (2007).
3. R. Reif, M. Wang, S. Joshi, O. A'Amar, and I. J. Bigio, "Optical method for real-time monitoring of drug concentrations facilitates the development of novel methods for drug delivery to brain tissue," *J. Biomed. Opt.* **12**(3), 034036 (2007).
4. A. Johansson, J. Svensson, N. Bendsoe, K. Svanberg, E. Alexandratou, M. Kyriazi, D. Yova, S. Gräfe, T. Trebst, and S. Andersson-Engels, "Fluorescence and absorption assessment of a lipid mTHPC formulation following topical application in a non-melanotic skin tumor model," *J. Biomed. Opt.* **12**(3), 034026 (2007).
5. A. Amelink, B. Kruijt, D. J. Robinson, and H. J. Sterenborg, "Quantative fluorescence spectroscopy in turbid media using fluorescence-DPS," *J. Biomed. Opt.* **13**(5), 054051 (2008).
6. A. Amelink and H. J. Sterenborg, "Measurement of the local optical properties of turbid media by differential path length spectroscopy," *Appl. Opt.* **43**(15), 3048–3054 (2004).
7. A. Amelink, H. J. Sterenborg, M. P. Bard, and S. A. Burgers, "*In vivo* measurement of the local optical properties of tissue by use of differential path length spectroscopy," *Opt. Lett.* **29**, 1087–1089 (2004).
8. R. L. van Veen, A. Amelink, M. Menke-Pluymers, C. van der Pol, and H. J. Sterenborg, "Optical biopsy of breast tissue using differential path length spectroscopy," *Phys. Med. Biol.* **50**(11), 2573–2581 (2005).
9. A. Amelink, O. P. Kaspers, H. J. Sterenborg, J. E. van der Wal, J. L. Roodenburg, and M. J. Witjes, "Noninvasive measurement of the morphology and physiology of oral mucosa by use of optical spectroscopy," *Oral Oncol.* **44**(1), 65–71 (2008).
10. B. C. Wilson, M. S. Patterson, and L. Lilge, "Implicit and explicit dosimetry in photodynamic therapy: a new paradigm," *Lasers Med. Sci.* **12**, 182–199 (1997).
11. D. J. Robinson, H. S. de Bruijn, N. van der Veen, M. R. Stringer, S. B. Brown, and W. M. Star, "Fluorescence photobleaching of ALA-induced protoporphyrin IX during photodynamic therapy of normal hairless mouse skin: the effect of light dose and irradiance and the resulting biological effect," *Photochem. Photobiol.* **67**, 140–149 (1998).
12. K. Woodburn, C. K. Chang, S. Lee, B. Henderson, and D. Kessel, "Biodistribution and PDT efficacy of a ketochlorin photosensitizer as a function of the delivery vehicle," *Photochem. Photobiol.* **60**, 154–159 (1994).
13. B. Aveline, T. Hasan, and R. W. Redmond, "Photophysical and photosensitizing properties of benzoporphyrin derivative monoacid ring A (BPD-MA)," *Photochem. Photobiol.* **59**, 328–335 (1994).
14. Q. Zhang, M. G. Müller, J. Wu, and M. S. Feld, "Turbidity-free fluorescence spectroscopy of biological tissue," *Opt. Lett.* **25**(19), 1451–1453 (2000).
15. M. G. Müller, T. A. Valdez, I. Georgakoudi, V. Backman, C. Fuentes, S. Kabani, N. Laver, Z. Wang, C. W. Boone, R. R. Dasari, S. M. Shapshay, and M. S. Feld, "Spectroscopic detection and evaluation of morphologic and biochemical changes in early human oral carcinoma," *Cancer* **97**(7), 1681–1692 (2003).
16. M. Canpolat and J. R. Mourant, "Monitoring photosensitizer concentration by use of a fiber-optic probe with a small source–detector separation," *Appl. Opt.* **39**, 6508–6514 (2000).
17. R. Weersink, M. S. Patterson, K. Diamond, S. Silver, and N. Padgett, "Noninvasive measurement of fluorophore concentration in turbid media with a simple fluorescence/reflectance ratio technique," *Appl. Opt.* **40**, 6389–6395 (2001).
18. B. W. Pogue and G. Burke, "Fiber-optic bundle design for quantitative fluorescence measurement from tissue," *Appl. Opt.* **37**, 7429–7436 (1998).
19. K. R. Diamond, M. S. Patterson, and T. J. Farrell, "Quantification of fluorophore concentration in tissue-simulating media by fluorescence measurements with a single optical fiber," *Appl. Opt.* **42**, 2436–2442 (2003).
20. S. Kascáková, B. Kruijt, H. S. de Bruijn, A. van der Ploeg-van den Heuvel, D. J. Robinson, H. J. Sterenborg, and A. Amelink, "*Ex vivo* quantification of mTHPC concentration in tissue: influence of chemical extraction on the optical properties," *J. Photochem. Photobiol., B* **91**(2–3), 99–107 (2008).
21. H. J. Jones, D. I. Vernon, and S. B. Brown, "Photodynamic therapy effect of m-THPC (Foscan) *in vivo*: correlation with pharmacokinetics," *Br. J. Cancer* **89**(2), 398–404 (2003).
22. P. Cramers, M. Ruevekamp, H. Oppelaar, O. Dalesio, P. Baas, and F. A. Stewart, "Foscan uptake and tissue distribution in relation to photodynamic efficacy," *Br. J. Cancer* **88**(2), 283–290 (2003).
23. L. Lilge, C. O'Carroll, and B. C. Wilson, "A solubilization technique for photosensitizer quantification in *ex vivo* tissue samples," *J. Photochem. Photobiol., B* **39**(3), 229–35 (1997).
24. B. Kruijt, H. S. de Bruijn, A. van der Ploeg-van den Heuvel, R. W. de Bruin, H. J. Sterenborg, A. Amelink, and D. J. Robinson, "Monitoring ALA-induced PpIX photodynamic therapy in the rat esophagus using fluorescence and reflectance spectroscopy," *Photochem. Photobiol.* **84**(6), 1515–1527 (2008).
25. J. C. Finlay and T. H. Foster, "Hemoglobin oxygen saturations in phantoms and *in vivo* from measurements of steady-state diffuse reflectance at a single, short source-detector separation," *Med. Phys.* **31**(7), 1949–1959 (2004).
26. O. P. Kaspers, H. J. Sterenborg, and A. Amelink, "Controlling the optical path length in turbid media using differential path length spectroscopy: fiber diameter dependence," *Appl. Opt.* **47**(3), 365–371 (2008).
27. J. C. Finlay, S. Mitra, and T. H. Foster, "*In vivo* mTHPC photobleaching in normal rat skin exhibits unique irradiance-dependent features," *Photochem. Photobiol.* **75**(3), 282–288 (2002).
28. A. Amelink, D. J. Robinson, and H. J. Sterenborg, "Confidence intervals on fit parameters derived from optical reflectance spectroscopy measurements," *J. Biomed. Opt.* **13**(5), 054044 (2008).

29. W. Alian, S. Andersson-Engels, K. Svanberg, and S. Svanberg, "Laser-induced fluorescence studies of meso-tetra(hydroxyphenyl)chlorin in malignant and normal tissues in rats," *Br. J. Cancer* **70**(5), 880–885 (1994).
30. R. Whelpton, A. T. Michael-Titus, R. P. Jamdar, K. Abdillahi, and M. F. Grahn, "Distribution and excretion of radio-labeled temoporfin in a murine tumor model," *Photochem. Photobiol.* **63**(6), 885–891 (1996).
31. H. J. Hopkinson, D. I. Vernon, and S. B. Brown, "Identification and partial characterization of an unusual distribution of the photosensitizer meta-tetrahydroxyphenyl chlorin (temoporfin) in human plasma," *Photochem. Photobiol.* **69**(4), 482–488 (1999).
32. M. Triesscheijn, M. Ruevekamp, R. Out, T. J. Van Berkel, J. Schellens, P. Baas, and F. A. Stewart, "The pharmacokinetic behavior of the photosensitizer meso-tetra-hydroxyphenyl-chlorin in mice and men," *Cancer Chemother. Pharmacol.* **60**(1), 113–122 (2007).
33. M. Kress, T. Meier, R. Steiner, F. Dolp, R. Erdmann, U. Ortmann, and A. Rück, "Time-resolved microspectrofluorometry and fluorescence lifetime imaging of photosensitizers using picosecond pulsed diode lasers in laser scanning microscopes," *J. Biomed. Opt.* **8**(1), 26–32 (2003).
34. K. R. Diamond, P. P. Malysz, J. E. Hayward, and M. S. Patterson, "Quantification of fluorophore concentration *in vivo* using two simple fluorescence-based measurement techniques," *J. Biomed. Opt.* **10**(2), 024007 (2005).